Theory and molecular dynamics modeling of spall fracture in liquids

A. Yu. Kuksin, G. E. Norman, V. V. Pisarev,* V. V. Stegailov, and A. V. Yanilkin
Joint Institute for High Temperatures of RAS, 13 bldg. 2. Izhorskaya str., 125412 Moscow, Russia
Moscow Institute of Physics and Technology, 9 Institutskii per., Dolgoprudnyy, 141700 Moscow region, Russia
(Received 11 May 2010; published 1 November 2010)

The model of fracture of liquid under tension is developed. It is based on the "nucleation-and-growth" approach introduced initially by D. R. Curran *et al.* [Phys. Rep. **147**, 253 (1987)]. The model derives the kinetics of fracture at mesoscale from the kinetics of elementary processes of void nucleation and growth in metastable liquid. The kinetics of nucleation and growth of voids in highly metastable liquid is studied in molecular dynamics (MD) simulations with the Lennard-Jones interatomic potential. The fracture under dynamic loading is considered, when the homogeneous void nucleation is relevant. The model is applied to the estimation of the spall strength of liquid. The growth of nanometer-size voids is shown to be well described by the Rayleigh-Plesset equation. The calculations of the void size distribution by the proposed kinetic model are in agreement with the distributions obtained in the direct large-scale MD simulations. The spall strength evaluated by the model is in a good agreement with the experimental data (the shock wave tests on hexane) and the direct MD simulations. The correspondence between our results on nucleation rate and the predictions of the classical nucleation theory is discussed.

DOI: 10.1103/PhysRevB.82.174101 PACS number(s): 64.60.Q−, 62.10.+s

I. INTRODUCTION

Metastable (stretched) liquids often appear during the operation of technical equipment.[1,2] Examples include hydraulic machines, water turbines, propellers, impulse heating of liquids by high-energy laser pulses,[3,4] or particle beams. Metastable liquid may appear in solids after an intense energy input. Examples include laser ablation[5,6] and shock-wave loading of solids.[7,8] The characteristic lifetimes of metastable liquids in different processes span from several picoseconds to several seconds. Complex description of such processes should include the models of metastable liquid behavior and decay. In the case of relatively slow processes (loading time $\tau \gtrsim 10^{-3}$ s), static strength criterion (cavitation threshold) is usually used.[9,10] At such time scales, fracture is usually initiated heterogeneously on the bubbles of gases and impurities in the liquid. In the case of very fast processes ($\tau \lesssim 10^{-6}$ s), static strength criteria are inapplicable. Such fast tension accompanies, e.g., shock-wave loading of liquids. Another example is melting of solids in the intense shockwaves. The melt is then exposed to the tension in the rarefaction wave. The strain rates in shockwave experiments reach 10^4-10^6 s^{-1}.[11–13] The strength of liquid depends on heterogeneous processes and on homogeneous void nucleation and growth as well. The fracture rate is determined by the initial concentration of impurities due to heterogeneous processes. At high strain rates, the liquid reaches high degree of metastability in a short time. That leads to the domination of homogeneous processes in fracture initialization as the homogeneous nucleation occur throughout the whole volume of liquid.

At present, two approaches are mainly used for describing and numerical modeling of fracture of liquids subjected to dynamic loading. In the first approach, fracture due to spontaneous void nucleation in liquid under negative pressure is considered. Fracture is supposed to occur when the nucleation rate exceeds some threshold value.[14] In the case of dynamic stretching, the threshold value of nucleation rate may depend on the strain rate.[11–13] This approach can be referred to as the nucleational approach. It is assumed that strength of liquid is determined solely by void nucleation kinetics. Usually the classic nucleation theory[1,2] is used in this approach to find the dependence of nucleation rate on pressure and temperature.

In the second, energetic approach[15] the energy change after formation of new surfaces in liquid during the dynamic tension is considered. Energy balance between the energy input during the deformation and energy consumption for the surface formation gives the minimal time needed for fragmentation and thus the minimal spall strength. In this approach, only energy balance is considered whereas elementary processes of void nucleation, growth, and coalescence are not considered explicitly. A similar approach is based on the consideration of momentum balance.[16] Due to the simplicity of final expressions for the spall time and the spall strength, this energetic spall criterion is often used for calculating the spall strength of liquid.[17,18]

Both approaches have certain drawbacks. As the nucleational approach does not take into account void growth, its usage for description of fracture in liquids with low viscosity is questionable. The energetic spall criterion gives only the minimal value of the spall strength assuming that there are enough centers of void nucleation present initially in a liquid.

Molecular dynamics (MD) method allows atomistic simulation of physical system behavior. It gives a possibility to perform a detailed study of fracture initiation during the dynamic loading.[19–22] Unfortunately, the system size in MD is now limited by 1 μm^3 and the simulation time is limited by several nanoseconds even for the high-end supercomputers. At strain rates typical for experiments, the characteristic time scales are microseconds and spatial scales are several cubic micrometers. Moreover, it seems to be difficult to extend the results of a single MD simulation to different loading conditions. We find more promising to incorporate the results of

multiple MD simulations into a higher-level fracture model in order to describe the macroscopic kinetics of fracture at the strain rates achievable in practice. One way to construct a multiscale fracture model is to take into account two processes: void nucleation in a stretched matter and their consequent growth. Such "nucleation-and-growth" (NAG) approach[23] is developed for modeling the fracture in solids. At the initial stage of fracture, void concentration is small so coalescence may not be taken into account.[24] Though this approach is more complicated than the two approaches above, it gives more detailed information about fracture kinetics. Also NAG approach allows to find not only the spall strength but also some other characteristics, for example, the size distribution of voids and detailed fracture kinetics for the arbitrary loading history.

The MD method allows us to study in detail the elementary processes of fracture: void nucleation and growth.[24] Kinetic characteristics of those processes obtained from MD simulations can then be incorporated into a fracture model.

The present work is devoted to the development of a model of fracture of liquid on the base of MD simulations. Preliminary results were published in Ref. 25. We consider the dynamic loading of liquid, when only the homogeneous processes are relevant to the fracture. Section II describes the direct MD simulations of the fracture evolution. The limitations of such an approach are discussed. Sections III and IV are devoted to the MD study of elementary fracture processes, void nucleation and void growth. In Sec. III, the technique of estimation of the nucleation rate from a series of MD simulations is presented and the correspondence between the results and the classical nucleation theory is discussed. In Sec. IV, the study of void growth in the MD system is presented. Section V is devoted to the development of a multiscale fracture model. The model is applied to the estimation of the spall strength of liquid hexane at a constant strain rate. The results of MD simulation and multiscale modeling are compared with the experimental data.

II. DIRECT MD SIMULATION OF FRACTURE AT HIGH STRAIN RATE

Direct MD simulations are performed to study and visualize the process of the liquid fracture at high strain rates. Liquid is represented by a Lennard-Jones (LJ) system with the potential

$$U(r) = 4\epsilon[(\sigma/r)^{12} - (\sigma/r)^6], \quad r < r_{cut}$$

with the cutoff radius $r_{cut}=4.0\sigma$. System with this potential reproduces well the properties of many simple liquids. Further, temperature, pressure, and other thermodynamic properties are given in reduced units: $T^*=kT/\epsilon$, $P^*=P\sigma^3/\epsilon$, $\rho^*=\rho\sigma^3/m$, $U^*=U/\epsilon$, where m is particle mass and k the Boltzmann constant. Time is given in units $\tau=(m\sigma^2/\epsilon)^{1/2}$.

The initial configuration for the simulation corresponds to the liquid phase at temperature $T^*=0.71$. The Langevin thermostat is used to maintain constant temperature during the MD run. Periodic boundary conditions are used to avoid surface effects. During the MD run the simulation box volume is changing at a constant given rate $\dot{\varepsilon}=\dot{V}/V_0$. Simulations are performed for several strain rates.

According to Ref. 26, the size L of a molecular dynamics system should be greater (or much greater) than the correlation length. In the case of fracture of liquid under tension, the apparent length scale is the average distance between voids. Thus, the system size should be chosen such that fracture is governed by the nucleation and growth of multiple voids. If the system size is insufficient, two effects are expected: overestimation of the spall strength and vanishing of the dependence of spall strength on strain rate.

The dependence of the sufficient system size on strain rate is estimated using the fracture model (which will be described further). The estimates show that the average distance between voids is inversely proportional to the strain rate. So, we should increase the size of MD system proportionally. The sufficient number of particles in the simulation is about 1 million for strain rates above $10^{-4}\tau^{-1}$ and about 10 million for strain rates $(1-2)\times10^{-5}\tau^{-1}$. In our simulations, the system contains 512 000 particles for simulations at strain rates above $3\times10^{-4}\tau^{-1}$ and 64 000 000 particles for the strain rates below $3\times10^{-4}\tau^{-1}$. Direct MD simulations for the strain rate $5\times10^{-6}\tau^{-1}$ would require 1 billion particles in the MD cell. Therefore, direct simulations for lower strain rates cannot be performed because of too long simulation times and too large system needed.

The degree of metastability increases with time under tension and voids appear in the cell (as the result of thermal fluctuations). If their size is larger than the critical size for the reached pressure, they continue growing. Figure 1 shows consequent snapshots of the simulation cell during the stretching. At some moment the rate at which empty volume increases due to void nucleation and growth becomes equal to the strain rate. The stress at this moment reaches its maximal value. This moment is considered as the spall moment, t_{sp}, and the value of stress is considered as the spall strength.

The dependence of spall strength on strain rate we obtained is shown in Fig. 2. To show the order of magnitude, reduced pressure units are converted in real pressure units using the Lennard-Jones potential parameters for liquid hexane:[27] $\epsilon/k_B=413$ K, $\sigma=5.909$ Å. For the comparison, the spall strength of liquid hexane under shockwave loading[11] is shown. At the strain rates higher than 3×10^8 s^{-1} the spall strength is nearly constant. Seemingly, at high strain rates system reaches the kinetic stability limit. The estimate of the thermodynamic stability limit of liquid phase, spinodal, is also shown. The spinodal lines poses the lower limit on the pressure at which thermodynamically and mechanically stable liquid can exist. In our simulations, kinetic stability limit lies close to the thermodynamic spinodal.

Figure 1 shows that the total empty volume at the moment when the stress reaches its maximal value is much less than the cell volume so there is no coalescence of voids yet. Thus, void nucleation in the volume and their growth can be considered as independent processes. This point is essential for the NAG model.

The system size needed for simulation scales as $\dot{\varepsilon}^{-3}$ and the time of fracture progress scales as $\dot{\varepsilon}^{-1}$. For that reason, the lower limit of the strain rate at which direct simulations

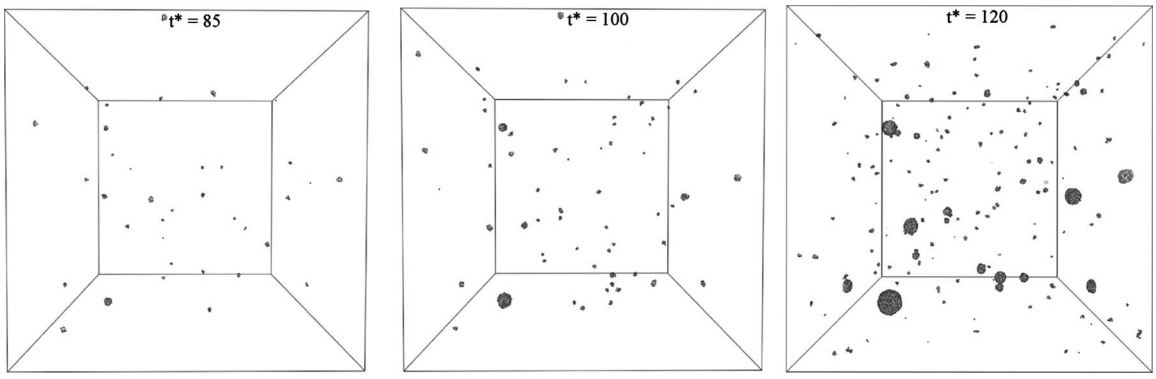

FIG. 1. Simulation cell snapshots. Only particles with excess potential energy $U^* > -3.0$ are shown. The snapshot at $t^* = 120$ corresponds to the moment when highest stress is reached.

can be performed, is about $10^{-4}\tau^{-1}$. In our simulations, we used 64 million particles for strain rate $10^{-4}\tau^{-1}$ and the simulation time was about 100τ or 10^5 steps. Thus, for direct simulations at strain rate $10^{-6}\tau^{-1}$ (close to ones attained in shockwave experiments) about 10 trillion particles are needed and the simulation time would be $10^4\tau$ or 10^7 steps. To find the spall strength at low strain rates, we used a two-level approach. The MD method was used to study void nucleation in a range of pressures and to determine the nucleation rate dependence on pressure and temperature. The growth kinetics of single voids was also studied in the MD simulations. The results were then incorporated into the kinetic fracture model, which was used to calculate the spall strength.

III. HOMOGENEOUS NUCLEATION

A. Simulation technique

Nucleation is an initial stage of a first-order phase transition. Homogeneous nucleation implies appearance of new phase nuclei in bulk volume of a single-phase system. The rate of a spontaneous phase transition is characterized by the nucleation rate, i.e., the average number of critical nuclei formed in unit volume per unit time.[1] It is calculated as $J = 1/(\langle t \rangle V)$, where $\langle t \rangle$ is the average lifetime of a homogeneous system and V the volume of the system. The technique we used to calculate the average lifetime was proposed in Refs. 28 and 29.

The initial states corresponding to the stretched liquid were obtained as follows. Initially particles in the simulation were arranged in the sites of simple cubic lattice and had randomly assigned velocities. Simple cubic lattice is unstable for the Lennard-Jones potential, so the system relaxes very quickly to the liquid state.

Then the liquid is equilibrated at a given temperature. The initial density of the liquid is chosen to give a negative pressure in the system. The main MD run starts from this state and a void nucleates at a random time during the run. The lifetime of the metastable phase is determined in a single run by the onset of the pressure increase which accompanies the void nucleation and growth process. The average lifetime of homogeneous phase is calculated by averaging lifetimes over an ensemble of MD runs corresponding to one macrostate.[28,30] In our case, macrostate is specified by a given temperature T^* and the pressure P^* in the system. As the systems of equations of motion for many particles are unstable, MD runs starting from a single initial state with slightly different integration steps diverge exponentially in time.[31] So, to create an ensemble of independent MD trajectories corresponding to one macrostate we carried out simulations with different steps from a single initial configuration.[28] The integration steps varied from $1.7 \times 10^{-3}\tau$ to $2.3 \times 10^{-3}\tau$.

If nucleation occurs randomly in the system and the average lifetime of the homogeneous phase does not depend on the moment we start the observation, then the lifetime distribution of trajectories corresponds to the law of exponential decay $n_{remain}(t) = n_0 \exp(-t/\langle t \rangle)$.[29,30,32] Figure 3 shows the correspondence between the results of MD simulations and the given stochastic model of nucleation. To analyze theoretically the dependence of the nucleation rate on pressure,

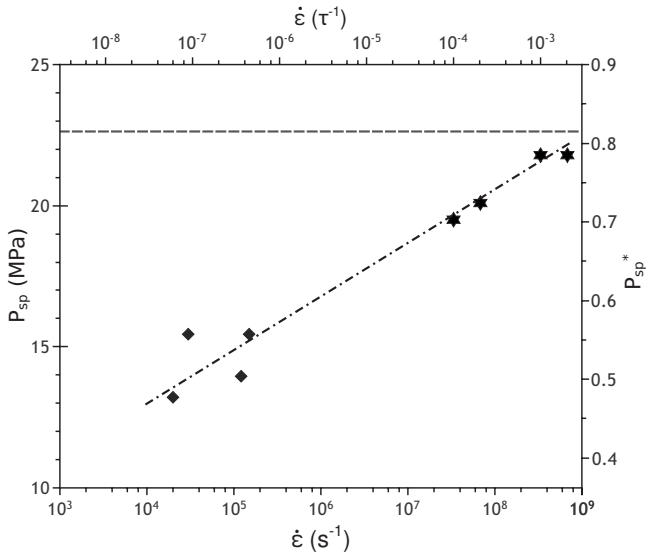

FIG. 2. Spall strength dependence on strain rate for the MD model of the Lennard-Jones liquid considered (stars), compared with the experimental data on liquid hexane by Utkin *et al.* (Ref. 11) (diamonds). Dashed line—the spinodal. Each MD point corresponds to one MD trajectory. The dashed and dotted line is a guide for an eye.

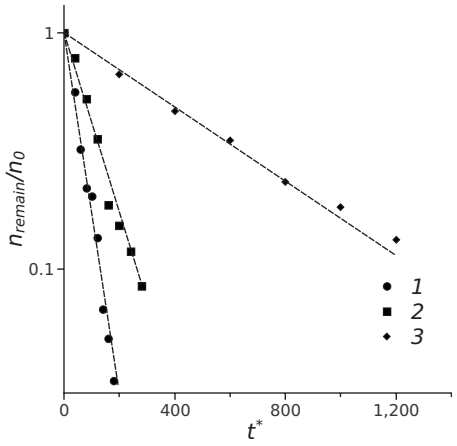

FIG. 3. Distribution of MD trajectories over lifetimes at $T^*=0.71$. $n_{remain}(t)$ is the number of trajectories in which nucleation has not occurred by the moment t; n_0 is the total number of performed MD runs for a given density. Dots show the simulation results: 1—$\rho^*=0.727$, $\langle t\rangle=57$; 2—$\rho^*=0.730$, $\langle t\rangle=110$; and 3—$\rho^*=0.740$, $\langle t\rangle=550$. Lines show the best fits by the exponential decay law.

we have to know the surface of tension of liquid.

B. Surface tension

We use two models to obtain the dependence of surface tension on temperature and curvature of surface. The first one presents the flat layer of liquid which is in equilibrium with its vapor.[33–35] The value of surface tension can be calculated from the forces acted on the boundaries of the simulation box. The results of surface tension of the flat surface are presented in Fig. 4(a). The increase in temperature leads to the decrease in the surface tension and it vanishes in the critical point. The results are in a good agreement with other calculations.[33,36] This approach, though, is usable only for flat surface or infinite curvature.

To obtain the dependence on curvature of surface we use the second model.[37,38] The liquid is relaxed at certain temperature and negative pressure. Then the void of the radius r is cut in the liquid and the stress relaxation is considered. If the radius of void is smaller than a critical size, the void collapses, if larger—it grows. There is a critical size of void corresponding to the unstable equilibrium. This size r_{equil} is connected with the surface tension and pressure by the Laplace equation: $\gamma=(P_{vapor}-P_{liquid})\cdot r_{equil}/2$

Figure 4(b) shows the dependences on the curvature of the surface for several temperatures. The values for the flat surface $1/r=0$ are given for the comparison. For large radius up to 2σ the surface tension decreases slowly and we must consider the dependence of surface tension on radius.[39,40] This dependence can be approximated by Tolman's formula:[41] $\gamma/\gamma_\infty=1/(1+2\delta/r)$ with parameter δ: $T=0.5,0.6,0.7-\delta\approx0.25\pm0.01$, $T=0.8-\delta\approx0.1$. We consider the equilibrium radius to obtain the value of surface tension. But the different radii corresponds to the different values of pressure. Pressure decreases with the decreasing of the radius and can influence on the surface tension. So we have two dependences of the surface tension. In this paper we are interested in the void nucleation process and we need this combined dependence to get the critical sizes of voids.

C. Dependence of nucleation rate on pressure and temperature

The dependence of nucleation rate on pressure is calculated for the isotherms $T^*=0.52$, $T^*=0.71$, $T^*=0.75$, and $T^*=0.8$ and shown in Fig. 5. The number of particles in a simulation cell varied from 8000 (high-J values) to 216 000 (low-J values). The classical homogeneous nucleation theory[1,2] predicts the dependence of the nucleation rate on pressure at a constant temperature in the form

$$J=J_0\exp\left(-\frac{W}{k_BT}\right), \tag{1}$$

where $W=\frac{16\pi\gamma^3}{3(P-P')^2}$ is the work of void formation, γ is the surface tension at the void-liquid interface, P is the pressure inside liquid, P' is the vapor pressure inside the void. The kinetic coefficient J_0 in Eq. (1) is defined by the kinetics of

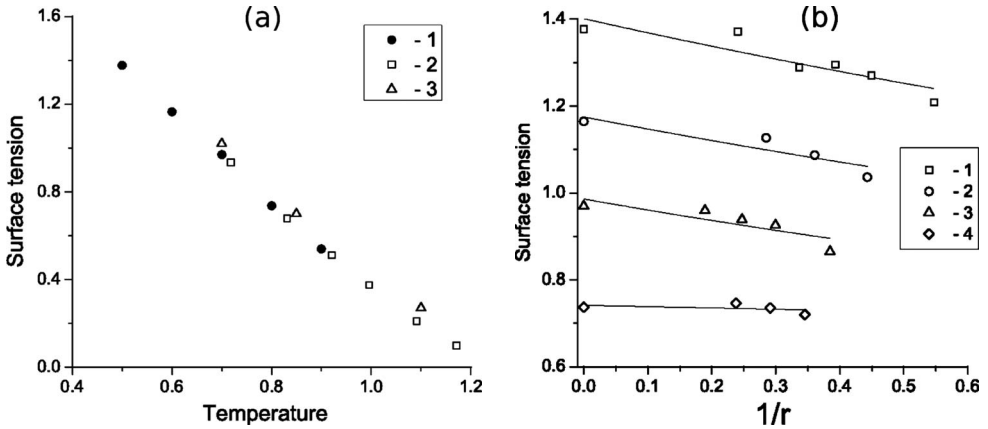

FIG. 4. (a) The dependence of surface tension γ of a flat surface on temperature T: solid circles—this work, open squares—Ref. 33, open triangles—Ref. 36. (b) The dependence of surface tension on curvature of surface for several temperatures T^*: squares—0.5, circles—0.6, triangles—0.7, and diamonds—0.8. The solid lines correspond to the approximation by the Tolman's formula with $\delta^*=0.24$ for $T^*=0.5$ and $T^*=0.6$, $\delta^*=0.26$ for $T^*=0.7$, $\delta^*=0.1$ for $T^*=0.8$.

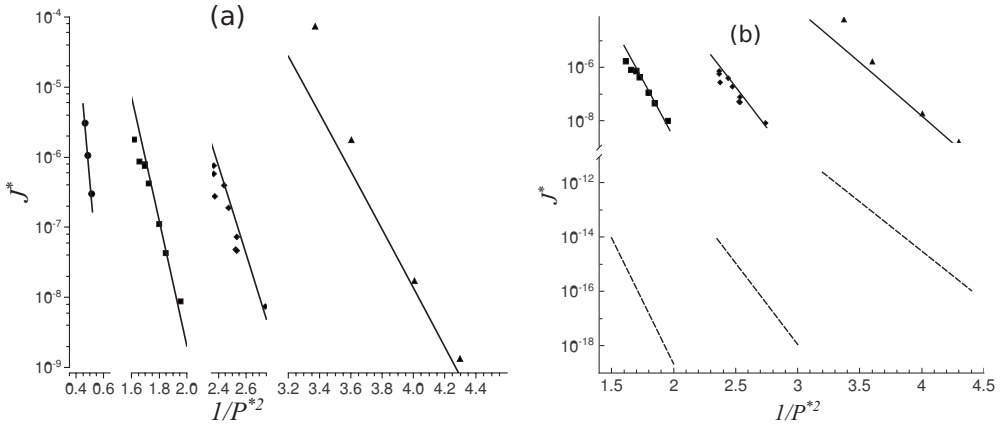

FIG. 5. The nucleation rate dependence on pressure and temperature on (a) large and (b) small scales. Circles—$T^*=0.50$; squares—$T^*=0.71$; diamonds—$T^*=0.75$; and triangles—$T^*=0.80$. Solid lines—calculations by Eq. (1) with $J_0=3\times10^5$ and pressure-dependent surface tension. Dashed lines—calculations by Eq. (1) with J_0 in form (2) and pressure-independent surface tension.

growth of near-critical voids. In the case of stretched liquid, classical theory gives the following expression:[14,42]

$$J_0(T) = \rho_l \frac{2\rho_l\gamma}{2\eta(P'-P)}\sqrt{k_BT\gamma}, \tag{2}$$

where ρ_l is the density of liquid and η is the dynamic viscosity coefficient.

When MD simulation results are compared with Eq. (1), pressure and temperature of liquid are considered to be equal to their mean values at the equilibrium section of MD trajectory. The pressure P' inside void is considered to be negligibly small compared to pressure P inside liquid. Indeed, the critical temperature for the Lennard-Jones system is $T^*_{cr}\approx1.3$.[43,44] The temperatures under consideration are substantially lower than T_{cr} therefore the pressure of saturated vapor is low and small voids are virtually empty.

The comparison between our simulation results and the predictions of the classical nucleation theory is shown in Fig. 5(b). The classical nucleation theory underestimates nucleation rates by many orders of magnitude. There are two reasons for that. First, in classical nucleation theory, the value of surface tension γ is usually assumed to be constant and equal to its value for the flat surface, γ_0. As shown in Sec. III A, the surface tension depends on bubble radius and it is lower for small bubbles. Thus, the classical nucleation theory overestimates the work of the critical bubble formation. In fact, in Eq. (1) we should assume $\gamma=\gamma[R_{cr}(P)]$. Second, Eq. (2) gives the value $J_0\sim1$ in the range $0.5<T^*<0.8$. The results of MD simulations in all temperature and pressure range can be fitted in form (1) assuming the surface tension dependent on pressure and with the preexponential factor $J_0=3\times10^5$. Seemingly, the approach used for J_0 calculation in the classical nucleation theory is not applicable for highly metastable liquids.

IV. VOID GROWTH

A. Simulations

The void growth kinetics is studied in MD experiments for isolated voids. To study the void growth in liquid, the following scheme is used. First, the system is equilibrated at a given temperature. Then, a spherical cavity is cut out the simulation box and the further MD simulation is performed. As the result we have the system with only one void with a known position. Such technique simplifies the diagnostics of void size. In order to calculate the cavity volume, the simulation box is covered by a grid of cells. Each cell contains two particles on average and the particles are represented as cubes with a size less than cell size. Empty cells are considered as "voids." The cavity volume equals to the total volume of the empty cells. The radius of the spherical cavity is given by the formula,

$$r(t) = \sqrt[3]{\frac{3}{4\pi}V_c(t)},$$

where $V_c(t)$ is the net volume of empty cells at the moment t.

Only the initial stage of the growth is studied while disturbance from the growing bubble has not crossed the boundaries of the simulation box. In this case, the growth of the bubble is the same as the expansion inside an infinite medium. Then the pressure increases and the conditions of the simulation do not correspond to the expansion inside infinite medium because of usage of periodic boundary conditions. To study void growth at long times, large simulation cells are used: $V=200\times200\times200a^3$, where a is the average distance between particles. Sound speed is $c_s=(\partial P/\partial\rho)^{1/2}\approx2\sigma/\tau$ in the pressure range under interest. With particle separation $a\sim\sigma$ the cell size we use allows to study void growth up to times 50τ. In order to compare the void growth kinetics with the theoretical model, we should know the viscosity as a function of pressure and temperature.

B. Viscosity

The values of viscosity are obtained by the model, proposed in Ref. 45. The main idea of the model is the artificial momentum flux. The flux is created by the momentum exchange between atoms in the opposite sides of calculation cell. It results in the opposite physical momentum flux and velocity gradient. We can calculate the value of the viscosity

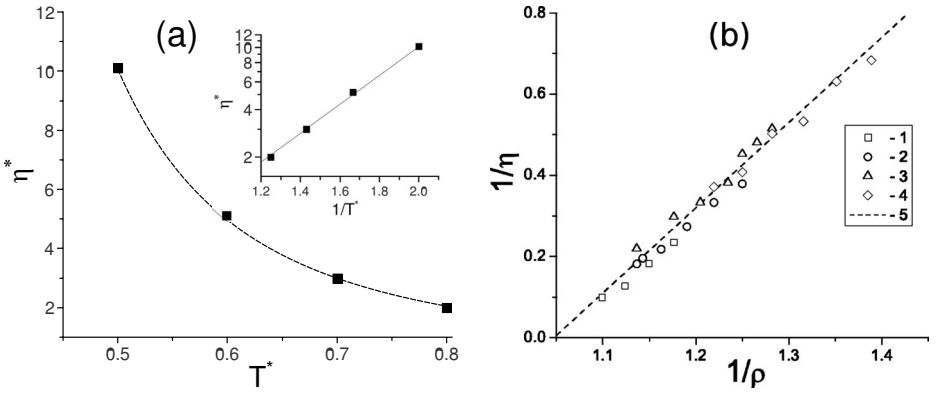

FIG. 6. The dependence of viscosity (a) on temperature at $P=0$ and (b) on density for four temperatures. (a) Squares—MD, dashed line—the approximation $\eta=0.145e^{2.12/T}$. (b) T^*: 1—0.5, 2—0.6, 3—0.7, 4—0.8, and the dashed line (5)—the general approximation $1/\eta=2.2/\rho-2.1$.

from Newton's law: $j(p_x)_z=-\eta\partial v_x/\partial z$. The calculated values of viscosity are shown in Fig. 6. There are two types of approximation in literature: Frenkel-Andrade (Arrhenius type) and Batchinski. The Frenkel-Andrade equation is based on the activation nature of momentum transfer and corresponds to the temperature dependence of viscosity,

$$\eta=\eta_0\exp\left(\frac{E}{RT}\right), \tag{3}$$

where E is the activation energy and η_0 is a constant. The dependence on temperature at $P=0$ is presented in Fig. 6(a). The data are approximated by formula (3) with $\eta_0=0.145$ and $E=2.12$.

The second approximation was found empirically by Batchinski,

$$\eta=\frac{c}{v_m-w}, \tag{4}$$

where $v_m=\rho_l^{-1}$ is the specific volume, c, w are constants. The results for different temperatures are shown in Fig. 6(b). They can be approximated by one curve in terms of the Eq. (4): $1/\eta=2.2/\rho-2.1$. There is no explicit dependence on temperature in this approximation. Temperature dependence is included in the dependence of ρ on the temperature along isobar $P=0$.

In our calculations we use the density dependence of viscosity $1/\eta=2.2/\rho-2.1$, that is a good approximation of the MD results for different temperatures.

C. Theoretical analysis

In the hydrodynamics, motion of void surface is described by the Rayleigh-Plesset equation[9]

$$R\ddot{R}+\frac{3}{2}\dot{R}^2+\frac{4\eta}{\rho}\frac{\dot{R}}{R}+\frac{2\gamma}{\rho R}=-\frac{P}{\rho}, \tag{5}$$

where η is the viscosity of liquid, γ the surface tension, and ρ the density.

With known viscosity, surface tension, and initial conditions, Eq. (5) can be solved. The initial conditions that correspond to the conditions in MD simulations are

$$R(0)=R_{cr},\quad \dot{R}(0)=0.$$

For void growth in metals, a simplified form of Eq. (5) is often used.[46] When the dominant terms are the viscosity and the pressure terms, we obtain the following relation:

$$4\eta\dot{R}/(\rho R)=-P/\rho. \tag{5'}$$

This equation has an apparent solution

$$R(t)=R_0\exp[-P/(4\eta)\cdot t]. \tag{6}$$

This relation is known as the law of viscous growth.

The comparison of the void growth kinetics in MD simulations and the corresponding solutions of Eq. (5) is shown in Fig. 7. The hydrodynamic approach describes the initial stage of void growth fairly well. Exact solution of Eq. (5) reveals asymptotically linear growth $R\sim\sqrt{-2P/3\rho}\cdot t$ at $t\to\infty$. Estimates show that void growth should be almost linear at $t\gtrsim 50\tau$. MD simulations also show nearly linear growth at $t\approx 50\tau$. Figure 7(b) shows that Eq. (6) is inappli-

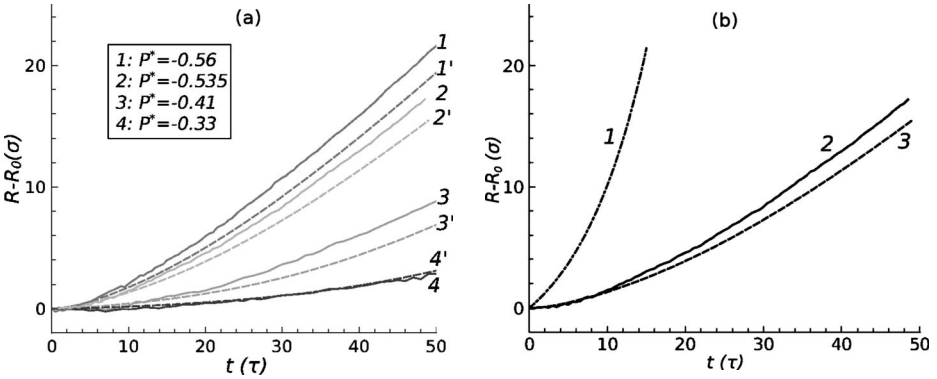

FIG. 7. Comparison of the MD simulations with (a) the Rayleigh-Plesset equation and (b) the law of viscous growth. (a) Solid lines—MD simulations, dashed lines—calculations by Eq. (5). (b) 1—viscous growth, Eq. (6); 2—MD simulation; and 3—calculations by Eq. (5).

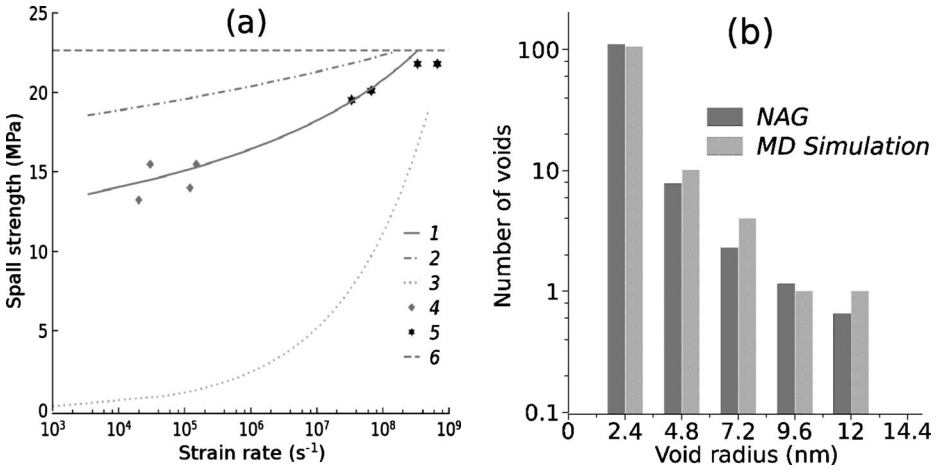

FIG. 8. (a) Spall strength dependence on strain rate for hexane. 1—NAG model calculations, 2—nucleational model calculations, 3—energetical spall criterion, 4—experimental data (Ref. 11), 5—direct MD simulations, and 6—spinodal. (b) Size distribution of voids in liquid hexane at the spall moment $t=t_{sp}$ for the strain rate $\dot{\varepsilon}=3\times10^8$ s^{-1}.

cable in the case of the Lennard-Jones liquid. Relation (6) gives the wrong asymptotics of the solutions. The viscous growth reveals a permanent acceleration of the void surface instead of the asymptotically linear growth. So, the fracture model should exploit the void growth kinetics derived from the Rayleigh-Plesset equation, in order to have the correct accounting of the void growth.

V. KINETIC FRACTURE MODEL

A. Model formulation

The proposed model for describing fracture in liquid is the development of the model presented in Ref. 24.

We assume the strain rate to be constant: $\dot{V}/V_0=\dot{\varepsilon}$ =const. The total volume of voids at a time t can be found as

$$V_{cav}(t)=\int_0^t v_{cav}(t-\tau)\dot{n}(\tau)d\tau,$$

where $v_{cav}(t-\tau)$ is the volume of one cavity appeared at moment τ and $\dot{n}(\tau)$ is the void nucleation rate in the volume V.

The volume of a single cavity and the nucleation rate can be expressed in terms of kinetics (homogeneous nucleation and growth rates) obtained from molecular dynamics simulations,

$$v_{cav}(t-\tau)=\frac{4}{3}\pi[R(t-\tau)]^3, \quad \dot{n}(\tau)=J[P(\tau)]V,$$

where $R(t-\tau)$ is void radius given by solution of Eq. (5).

We take the spall time t_{sp} as the time when the rate of the increase in the volume of voids is equal to the strain rate: $\frac{1}{V_0}\frac{dV_{cav}}{dt}(t_{sp})=\dot{\varepsilon}$. Using the given dependence $P(t)$, we obtain the achievable pressure at the spall time, i.e., the spall strength. This spall criterion is consistent with the spall criterion for direct MD simulations (maximal stress).

To find the pressure dependence on time, the expression $P(t)=P[\rho_0/(1+\dot{\varepsilon}t),T]$ is used. Here $P(\rho,T)$ is the equation of state of the liquid. Temperature is supposed to be constant and pressure $P(\rho)$ along isotherms is calculated by MD method.

B. Modeling results

Figure 8(a) shows spall strength calculated by the proposed model, along with the spall strength of hexane in direct MD simulations and experimental data.[11] A good agreement of the NAG model results with the experimental data and the direct MD simulation results proves the applicability of the proposed model to the fracture description at experimentally attainable strain rates.

Our model predicts that at the strain rate $\dot{\varepsilon}\approx3\times10^8$ s^{-1} the spall strength reaches the spinodal strength of the LJ liquid. It means that at higher strain rates the spall strength should show no dependence on strain rate. In the direct MD simulations spall strength is independent on strain rate for $\dot{\varepsilon}>3\times10^8$ s^{-1}.

The comparison of the calculated void size distribution with the one obtained in the direct MD simulations is the direct verification of the NAG model predictions. The void size distributions at the spall moment for strain rate $\dot{\varepsilon}=6\times10^7$ s^{-1} are shown in Fig. 8(b). The calculations show very good agreement with the direct simulations. There are several large voids along with many small ones. One should note that the volume of large voids is larger than the summary volume of small voids. Thus, the growth of voids appeared at the initial stages gives essential contribution to fracture kinetics, comparable with the void nucleation just before the spall moment.

The spall strength calculated without accounting of void growth [i.e., under assumption $R(t)=R_{cr}$] is shown in Fig. 8(a) with the dashed and dotted line. Such a simplification of the NAG model gives an overestimate of spall strength of ~20%. As shown above, large voids with size much more than critical radius account for the maximal fraction of the empty volume. Fracture occurs not only due to nucleation of new voids but due to void growth too. Modeling results show that taking into account the void growth diminishes the spall strength significantly.

The spall strength calculated using the energetic spall criterion[15] is shown in Fig. 8(a) with the dashed line. In this case, spall strength is given by the formula,

$$P_{sp}=(6\rho^2c_s^3\gamma\dot{\varepsilon})^{1/3}, \quad (7)$$

where ρ is the liquid density, c_s is the sound speed, and γ is the surface tension. The values of the spall strength calcu-

lated using the energetic spall criterion are several times lower than experimentally observed values. When expression (7) is derived, the limiting case is implied: all the energy that has been put in the liquid by stretching is spent on the new surface formation. This assumption may be correct when there is a sufficient number of void nucleation centers (gas microbubbles, solid includings, etc.) present in the liquid initially. In our case the homogeneous void nucleation in liquid seems to be the limiting stage of spallation. All the energy is not spent on the new surface formation and this leads to the increase in the spall strength compared to Eq. (7).

C. Spall strength dependence on the strain rate

The dependence of the spall strength on the strain rate for the NAG model and the nucleational model is well approximated by the formula $P_{sp} \simeq A/\sqrt{\ln(B/\dot{\varepsilon})}$. In the case of the nucleational model this dependence may be derived from the classical theory of homogeneous nucleation under the assumption that the average volume of the nucleus depends weakly on pressure.[11]

This relation is also valid for NAG model. Below we present a simplified analytical model which accounts for such a form of dependence. The rate of volume increase for a void of radius R is

$$\dot{v}_{cav}(\tau) = 4\pi R^2(\tau)\dot{R}.$$

For N identical voids we have

$$\dot{V}_{cav} = 4\pi R^2 \dot{R} \cdot N.$$

The number $dN = \dot{n}(t)dt$ of voids appear in the time interval $(t;t+dt)$. The rate of their volume increase at the spall time moment (i.e., the time of growth is $t_{sp}-t$) is

$$d\dot{V}_{cav}(t) = \dot{v}_{cav}(t_{sp}-t) \cdot dN(t) = 4\pi[R(t_{sp}-t)]^2 \dot{R}(t)\dot{n}(t)dt,$$

where $\dot{n}(t)$ is the void nucleation rate at the time t, $R(t_{sp}-t)$ is the void radius at the time t_{sp}, and $\dot{R}(t)$ is the void growth rate.

The void nucleation rate increases sharply as the stress increases. Thus a large difference in the rates of increase in empty volume (that "compensates" the effect of the strain rate) can be attained by small change in stress. It means that the spall strength should depend on the strain rate only weakly: $P_{sp} \approx$ const. Then we assume for simplicity the linear dependence of pressure on time,

$$P(t) = -K_T \rho_0 \dot{\varepsilon} t,$$

where K_T is bulk modulus of liquid. Then relation $P_{sp} \approx$ const means that $\dot{\varepsilon} t_{sp} \approx$ const. At $t \approx t_{sp}$ the void growth rate $\dot{R} \simeq \dot{R}(t_{sp}) = \mu_0$ and the void radius $R(t_{sp}-t) \approx \mu_0(t_{sp}-t)$. Thus we have

$$d\dot{V}_{cav}(t) \approx 4\pi[\mu_0(t_{sp}-t)]^2 \mu_0 \dot{n}(t)dt.$$

The void nucleation rate in volume V is

$$\dot{n}(t) \propto J[P(t)] \propto \exp\left[-\frac{b^2}{P^2(t)}\right] \propto \exp\left(-\frac{a^2}{t^2}\right).$$

Now we make a simplification. We assume that the voids which account for fracture appear in a narrow time interval $(t_m; t_m+\Delta t)$ and then their growth occurs. Really, there is a distribution of void sizes. Because of the sharp dependence of the nucleation rate on pressure too few voids nucleate at early times to affect significantly on the empty volume. On the other side, voids which appear at moments close to the spall moment are very small at this moment. Thus, they do not give significant contribution to the rate of increase in empty volume either. So, the voids which give a significant contribution to the rate of increase in empty volume nucleate around some moment $t_m < t_{sp}$. Assume that for all strain rates $t_m/t_{sp} = \alpha \approx$ const and $\Delta t/t_{sp} = \delta \approx$ const. Then the total number of voids is

$$N = \dot{n}(t_m)\Delta t = J(t_m)V_0 \Delta t \propto \exp\left[-\frac{b^2}{P^2(t_m)}\right] \cdot \delta \cdot t_{sp}$$

and the fracture rate at the spall moment

$$\frac{\dot{V}_{cav}(t_{sp})}{V_0} = N \cdot 4\pi[\mu_0(1-\alpha)t_{sp}]^2 \mu_0 \propto t_{sp}^3 \exp\left[-\frac{b^2}{P^2(t_m)}\right].$$

Having the spall criterion $\frac{1}{V_0}\frac{dV_{cav}}{dt}(t_{sp}) = \dot{\varepsilon}$ and the requirement $\dot{\varepsilon} t_{sp} \approx$ const we conclude that

$$\exp\left[-\frac{b^2}{P^2(t_m)}\right] = \left(\frac{\dot{\varepsilon}}{B}\right)^4.$$

That gives an expression for the spall strength $P_{sp} = t_{sp}/t_m \cdot P(t_m) \simeq t_{sp}/t_m \cdot b/2\sqrt{\ln(B/\dot{\varepsilon})}$ (where B is a constant), that is, the spall strength dependence on strain rate has the same form as in the nucleational model. In this simplified model $b^2 \simeq 16\pi\gamma^3/3k_BT$. For $T=292$ K MD simulations give $\sqrt{16\pi\gamma^3/3k_BT} = 96$ MPa. The calculations by the proposed equation coincide with the curve 1 in Fig. 8 if we take $b=115$ MPa and $B=2.1\times10^{11}$ s^{-1} so the simple estimate of the value of b is reasonable. We can also conclude that the voids which give the main contribution to the spall form about at $t_m \sim 0.8 t_{sp}$.

Such a weak dependence of the spall strength on the strain rate results from a very strong dependence of nucleation rate on pressure. A several percent increase in stress leads to a several orders of magnitude increase in the nucleation rate. Thus an order of magnitude change in strain rate changes spall strength just by several percent.

VI. CONCLUSIONS

A mechanism of fracture in liquid under dynamic loading comprising homogeneous void nucleation and growth is considered. Fracture of the Lennard-Jones liquid is studied in the large-scale MD simulations (64 million atoms) and MD simulations of elementary processes of void nucleation and growth. On the basis of the MD simulation results, a model of fracture is proposed which allows to extend the spatial and temporal scales of the modeling in comparison with direct

MD simulations. Using this model, the spall strength of liquid under high strain rates is calculated. For the comparison of the results with the available experimental data, parameters of the Lennard-Jones potential for the liquid hexane are used. (1) The large-scale MD simulations of fracture process in the Lennard-Jones liquid are performed for the strain rates $10^{-4}-2\times10^{-3}\tau^{-1}$ and the spall strength is calculated. The spall strength is nearly constant at strain rates higher than $10^{-3}\tau^{-1}$. It is shown that maximal stress in liquid is reached while voids appeared still do not coalesce. The void size analysis shows that fracture occurs not only through nucleation of new voids just before the spall moment but also through the growth of voids that have appeared earlier.

(2) The kinetics of void nucleation is studied in the MD simulations. The results are compared with the classical nucleation theory. The dependence of the nucleation rate on pressure calculated from the MD simulations shows that the work of the critical void formation can be expressed through the surface tension in the same way as in the classical theory. But the surface tension value itself depends on the radius of the critical void.

(3) The void growth is simulated. The kinetics of void growth obtained is well described by the Rayleigh-Plesset equation.

(4) The data obtained for the nucleation rates and void growth are incorporated in a model of fracture based on the NAG approach. The spall strength of the liquid hexane at a constant strain rate is calculated using the proposed model. The NAG model reproduces the direct MD simulation results on spall strength at strain rates 10^7-10^9 s^{-1}. The void volume distribution at the spall moment calculated in the NAG model is in a good agreement with the one obtained in the direct MD simulations. At strain rates 10^4-10^5 s^{-1} the NAG model gives the results well consistent with the experimental data.

(5) For the comparison, the nucleational fracture model and the energetic spall criterion are applied to calculate the spall strength. They are shown to give incorrect results on spall strength of liquids. In nucleational model void growth is not taken into account but this factor is crucial for the fracture description. The energetic spall criterion does not consider homogeneous void nucleation as the limiting stage of spallation and gives a large underestimate of the spall strength.

ACKNOWLEDGMENTS

This work is partially supported by the RAS under Programs No. 2 (coordinator V. E. Fortov), No. 13 (G. I. Savin), No. 14 (Yu. I. Zhuravlev), No. 22 (N. F. Morozov), and No. OE 12 (D. M. Klimov) and RFBR under Grants No. 09-08-12161-ofi-m and No. 09-08-01116-a. V.V.P. acknowledges the financial support of the "Dynasty" foundation. MD simulations are performed using the LAMMPS package (Ref. 47) on the clusters of the Joint Supercomputer Center of RAS (MVS-100K) and Moscow Institute of Physics and Technology (MIPT-60).

*pisarevvv@gmail.com

[1] V. P. Skripov, *Metastable Liquids* (Wiley, New York, 1974).
[2] P. Debenedetti, *Metastable Liquids: Concept and Principles* (Princeton University Press, Princeton, NJ, 1996).
[3] S. I. Kudryashov, K. Lyon, and S. D. Allen, Phys. Rev. E **73**, 055301 (2006).
[4] S. I. Kudryashov, K. Lyon, and S. D. Allen, Phys. Rev. E **75**, 036313 (2007).
[5] N. A. Inogamov, V. V. Zhakhovskii, S. I. Ashitkov, Y. V. Petrov, M. B. Agranat, S. I. Anisimov, K. Nishihara, and V. E. Fortov, J. Exp. Theor. Phys. **107**, 1 (2008).
[6] D. S. Ivanov and L. V. Zhigilei, Phys. Rev. B **68**, 064114 (2003).
[7] G. Kanel, S. Razorenov, A. Utkin, and D. Grady, *Shock Compression of Condensed Matter 1995*, AIP Conf. Proc. No. 370 (AIP, New York, 1996), p. 503.
[8] T. de Rességuier, L. Signor, A. Dragon, P. Severin, and M. Boustie, J. Appl. Phys. **102**, 073535 (2007).
[9] C. Brennen, *Cavitation and Bubble Dynamics* (Oxford University Press, New York, 1995).
[10] D. D. Joseph, Phys. Rev. E **51**, R1649 (1995).
[11] A. V. Utkin, V. A. Sosikov, and A. A. Bogach, J. Appl. Mech. Tech. Phys. **44**, 174 (2003).
[12] A. V. Utkin and V. A. Sosikov, J. Appl. Mech. Tech. Phys. **46**, 481 (2005).
[13] A. A. Bogach and A. V. Utkin, J. Appl. Mech. Tech. Phys. **41**, 752 (2000).
[14] V. E. Vinogradov and P. A. Pavlov, High Temp. **38**, 379 (2000).
[15] D. Grady, J. Mech. Phys. Solids **36**, 353 (1988).
[16] A. A. Gruzdkov and Y. V. Petrov, Tech. Phys. **53**, 291 (2008).
[17] M. Povarnitsyn, K. Khishchenko, and P. Levashov, Int. J. Impact Eng. **35**, 1723 (2008).
[18] M. E. Povarnitsyn, T. E. Itina, M. Sentis, K. V. Khishchenko, and P. R. Levashov, Phys. Rev. B **75**, 235414 (2007).
[19] J. Belak, J. Comput.-Aided Mater. Des. **5**, 193 (1998).
[20] J. Belak, J. Comput.-Aided Mater. Des. **9**, 165 (2002).
[21] A. Y. Kuksin, G. E. Norman, V. V. Stegailov, A. V. Yanilkin, and P. A. Zhilyaev, Int. J. Fract. **162**, 127 (2010).
[22] V. V. Stegaĭlov and A. V. Yanilkin, Sov. Phys. JETP **104**, 928 (2007).
[23] D. R. Curran, L. Seaman, and D. A. Shockey, Phys. Rep. **147**, 253 (1987).
[24] A. Y. Kuksin and A. V. Yanilkin, Dokl. Phys. **52**, 186 (2007).
[25] A. Y. Kuksin, G. E. Norman, V. V. Pisarev, V. V. Stegailov, and A. V. Yanilkin, High Temp. **48**, 511 (2010).
[26] A. Y. Kuksin, I. V. Morozov, G. E. Norman, V. V. Stegailov, and I. A. Valuev, Mol. Simul. **31**, 1005 (2005).
[27] *Spravochnik Himika*, edited by B. P. Nikol'skiy (Himiya, Moscow, Leningrad 1966), Vol. 1 (in Russian).
[28] G. E. Norman and V. V. Stegailov, Dokl. Phys. **47**, 667 (2002).
[29] G. E. Norman and V. V. Stegailov, Mol. Simul. **30**, 397 (2004).
[30] T. T. Bazhirov, G. E. Norman, and V. V. Stegailov, J. Phys.: Condens. Matter **20**, 114113 (2008).

[31] G. E. Norman and V. V. Stegailov, Sov. Phys. JETP **92**, 879 (2001).
[32] V. P. Skripov and V. P. Koverda, *Spontaneous Crystallization of Supercooled Liquids* (Nauka, Moscow, 1984) (in Russian).
[33] V. Baidakov, G. Chernykh, and S. Protsenko, Chem. Phys. Lett. **321**, 315 (2000).
[34] G. V. Kharlamov, A. A. Onischuk, P. A. Purtov, S. V. Vosel, and A. V. Bolesta, Atmos. Oceanic Opt. **21**, 679 (2008).
[35] G. V. Kharlamov, A. A. Onischuk, P. A. Purtov, S. V. Vosel, and A. V. Bolesta, e-J. Surf. Sci. Nanotechnol. **8**, 197 (2010).
[36] M. Mecke, J. Winkelmann, and J. Fischer, J. Chem. Phys. **107**, 9264 (1997).
[37] Z. Insepov, A. Hassanein, T. Bazhirov, G. Norman, and V. Stegailov, Fusion Sci. Technol. **52**, 885 (2007).
[38] S. H. Park, J. G. Weng, and C. L. Tien, Int. J. Heat Mass Transfer **44**, 1849 (2001).
[39] D. I. Zhukhovitskii, Colloid J. **65**, 440 (2003).
[40] J. W. P. Schmelzer, I. Gutzow, and J. Schmelzer, Jr., J. Colloid Interface Sci. **178**, 657 (1996).
[41] R. Tolman, J. Chem. Phys. **17**, 333 (1949).
[42] Y. Kagan, Zh. Fiz. Khim. **XXXIV**, 92 (1960).
[43] A. Y. Kuksin, G. E. Norman, and V. V. Stegailov, High Temp. **45**, 37 (2007).
[44] V. G. Baidakov and S. P. Protsenko, Phys. Rev. Lett. **95**, 015701 (2005).
[45] F. Müller-Plathe, Phys. Rev. E **59**, 4894 (1999).
[46] E. Dekel, S. Eliezer, Z. Henis, E. Moshe, A. Ludmirsky, and I. Goldberg, J. Appl. Phys. **84**, 4851 (1998).
[47] S. Plimpton, J. Comput. Phys. **117**, 1 (1995).